

## Biological Synthesis of Silver Nanorods from *Nocardia mediterranei*-5016 and its Antitumor Activity against Non-small cell lung carcinoma cell line

R. Subbaiya<sup>1\*</sup>, M. Masilamani Selvam<sup>2</sup>, K. Sundar<sup>3</sup>

<sup>1</sup>Department of Biotechnology, K.S.Rangasamy College of Technology, Tiruchengode, Namakkal (dt), TamilNadu, India.

<sup>2</sup>Department of Biotechnology, Sathyabama University, Chennai, India.

<sup>3</sup>Department of Food Science and Technology, Pondicherry University, Puducherry, India.

**Abstract:** In this experiment we optimized that 1mM concentration of silver nitrate was required for biological synthesis by inoculating the pellet and supernatant obtained from *Nocardiamediterranei* in various concentration of silver nitrate solution. The UV Spectrophotometer revealed the quantitative formation of silver nanorods. The characteristics of obtained silver nanorods were studied using Fourier Transform Infrared Spectroscopy (FT-IR), scanning electron microscopy (SEM) and transmission electron microscopy (TEM) analysis. Antibacterial activity of silver nanorods produced by *Nocardia mediterranei* was checked with the help of test microorganisms. The anticancerous activity against Non-small cell lung carcinoma cell line (NCI-H460) by MTT assay reveals 12.52 $\mu$ g (IC<sub>50</sub>) inhibits the NCI-H460 growth. The effect of nanoparticles on cell morphology was obtained by Hoechst staining to confirm the cell death. The DNA damage in the treated cells was evaluated using single-cell gel electrophoresis (comet) assay. DNA was observed in cells treated with nanoparticles after 24hrs incubation were as percentage of damaged cells increased on treatment with this compound for 48hrs, which was shown by the prominent comets with tail. Increased ROS generation during nanoparticle treatment showed an additive effect of this particle in NCI-H460 cells.

**Keywords:** *Nocardia mediterranei*, Antitumor Activity, Hoechst, Comet assay, ROS.

### 1. Introduction

Nanoscience and technology is an emerging area research which dealing about the nanoscale materials usually ranging from 1 to 100 nanometers (nm). These nanomaterials are helpful to solve the challenges in the area of fuel cell, solar cell, health issue, medicine, catalysis, water treatment and many more. [1,2]. Nanomaterials having very high surface to volume ratio hence often show unique and considerably changed physical, chemical and biological properties compared to their macro scaled counterparts [3]. Nobel metal nanoparticles gold, silver, and copper have been used mostly for the synthesis of stable dispersions of nanoparticles, which are useful in areas such as photography, catalysis, biological labeling, photonics, optoelectronics and Surface-Enhanced Raman Scattering (SERS) detection [4,5].

Silver nanoparticles have proven to be effective is in controlling and suppressing bacterial growth. There have already been developed several applications which use the bactericidal effect of silver nanoparticles [6]. In addition characterization of the nanoparticles to examine size, shape, and quantity is important. A number of different measurement techniques can be used for this purpose, including Atomic Force Microscopy (AFM), Scanning Electron Microscopy (SEM), Absorbance Spectroscopy and Dynamic Light Scattering (DLS) [7]. Cancer is the third leading cause of death (after heart disease and stroke) in developed countries and the

second leading cause of death [8]. Several nanotechnological approaches have been used to improve delivery of chemotherapeutic agents to cancer cells with the goal of minimizing toxic effects on healthy tissues while maintaining antitumour efficacy [9]. The ability to control and manipulate the accumulation of nanoparticles for an extended period of time inside a cell can lead to improvements in diagnostic sensitivity and therapeutic efficiency [10].

## 2. Materials and Methods

### 2.1. Materials

*Nocardia mediterranei*-5016 culture was obtained from NCIM, Pune, India. The obtained species was inoculated in MGYM media which acts as growth media for its growth and proliferation. Culture was grown in Yeast malt broth at 37°C for 7 days. The lyophilized culture was added to the broth in Laminar air flow chamber. The flasks were incubated in the shaking incubator at 200 RPM for 7 days [11].

### 2.2. Synthesis and characterization of silver nanorods

The various concentration of Silver Nitrate solution viz, 0.5mM, 1.0mM, 1.5 mM, 2.00 mM and 2.5 mM were taken as 2 sets in 100 ml Erlenmeyer flask. Distilled water was used through out the experiment. To one set, 5 ml of culture (*Nocardia mediterranei*-5016) was added in each flask and to the other set, 5 ml of supernatant was added. This was kept for incubation for 20 days in dark condition. The UV spectrophotometer reading was taken at 400-450 nm. The concentration at which maximum absorbance got was observed.

From the inoculated solution kept for incubation, 1ml of solution is taken aseptically and reading was taken in UV Spectrophotometer (Hitachi U 2900). The wavelength scanning was performed every 24 hours interval and the peak obtained was observed. The peaks observed within the range of 300-700 nm. Overnight freeze dried sample were lyophilized by lyophilizer (LARK Penguin Classic Plus). Characterization was done with Fourier Transform infrared (FT-IR) spectroscopy (IR Affinity, Shimadzu) analysis was made. All measurement were carried out in the range of 500 – 3500cm<sup>-1</sup> at a resolution of 4 cm<sup>-1</sup>. Scanning electron microscope (Jeol 6390;Hitachi;Japan) and Transmission Electron Microscopy (TEM) were used to obtain the surface image and the size of the microbially synthesized silver nanoparticle.

### 2.3. *In Vitro* Study of Anticancerous Activity:

#### 2.3.1. Chemicals

3-(4,5-dimethyl thiazol-2yl)-2, 5- agarose were obtained from Hi-Media Laboratories Ltd, Mumbai, India. Ethidium bromide, Hoechst 33258, dimethyl sulphoxide (DMSO) and were obtained from Sigma Aldrich Chemicals Co, USA. The rest of the chemicals and solvents utilized were of analytical grade and obtained from Hi-Media Laboratories Ltd., Mumbai, India. RPMI 1640 medium with glutamine and without sodium bicarbonate was obtained from Sigma Aldrich Chemicals Co, USA. Fetal bovine serum was used for the growth of cells and was obtained from Sigma Aldrich Chemicals Co, USA. Penicillin and streptomycin were obtained from Hi-Media Laboratories Ltd, Mumbai, India. Tissue culture flasks, tissue culture plates, centrifuge tubes etc., were obtained from chemico glass and scientific company, Erode.

#### 2.3.2. Maintenance of Cells:

Human non-small cell lung carcinoma cell line (NCI-H460), were grown as monolayer in RPMI 1640 medium with 10% FBS and 2% antibiotics. Stock cultures were sub-cultured every 7<sup>th</sup> day after harvesting the cells with trypsin-EDTA and then seeding them in tissue culture flask to maintain in exponential phase. Non-small cell lung carcinoma cell line (NCI-H460) used in the present study were procured from National Centre for Cell Science (NCCS), Pune, India.

#### 2.3.3. Cell Counting, Reagents and Equipments:

0.04% trypan blue in PBS, haemocytometer and inverted microscope. The cell suspension was mixed gently and an aliquot was added to the trypan blue solution-I (100 • 1 cellsuspension: 100 • 1 dye) and was then counted in haemocytometer.

**Calculations:**

Total No of viable cells =  $A \times B \times C \times 10^4$

Total dead count =  $A \times B \times D \times 10^4$

Total cell count = Viable cell count + dead cell count

% Viability =  $\frac{\text{Viable cell count} \times 100}{\text{Total cell count}}$

where, A = volume of cells

B = dilution factor in trypan blue

C = mean number of unstained cells

D = mean number of dead cells or stained cells  $10^4$  is the conversion factor for  $0.1\text{mm}^3$  to 1 ml

**2.4. MTT Assay:**

The cytotoxicity effect of different size of nanoparticles were determined by method of Mosmann *et al.* (1983).

**Reagents:** MTT stock solution (5mg/ml), MTT - 50 mg and was dissolved in 10 ml of PBS, After vortexing for 20 minutes, it was filtered through 0.45 micron filter [12]. The bottle was wrapped with aluminium foil or paper to block light, as MTT is light-sensitive. The preparation was stored at  $4^\circ\text{C}$  [13].

NCI-H460 cells were seeding ( $5 \times 10^3$  cells/well) in 96 well microtiter plate for 24h. The plates were incubated with nanoparticles at different concentrations ( $2\mu\text{g}$ - $20\mu\text{g}$ ) for 24h, 48h and 72h respectively (In each concentration six replicates were processed ( $n = 6$ )) [14]. The medium was refreshed and  $20\mu\text{l}$  of MTT solution (5mg/ml) was added. The plates were incubated for 3h in dark. The formazan crystals developed were solubilized using  $100\mu\text{l}$  of DMSO. The colour developed was measured in an ELISA reader (Bio Rad, USA) at wavelength 570 nm with a reference wavelength at 630 nm.

**Analysis:** A graph of absorbance (Y-axis) against the concentration of the drug (X-axis) was plotted and  $\text{IC}_{50}$  concentration was determined as the dye concentration that was required to reduce the absorbance to half that of control. The data was then converted to percentage inhibition curve, to normalize a series of curves.

**2.5. Assessment of Cell Morphology, Hoechst 33258 Staining, Stock Solution:**

**Working Solution:** 1 mg of Hoechst 33258 was added to 1 ml of PBS buffer.  $5\mu\text{l}$  of stock solution was taken and the volume was made up to  $500\mu\text{l}$  using distilled water. NCI-H460 cells were grown in 6 well plates ( $5 \times 10^3$  cells/well) for 24h. The cells were then incubated with the  $\text{IC}_{50}$  dose of different size of nanoparticles for 24h and 48h. The medium was discarded and the cells were washed with PBS. The cells were then trypsinized and placed on a glass slide and stained with acridine orange, ethidium bromide and the Hoechst stain [15]. The cells were then viewed in a fluorescent microscope (Carl Zeiss, Jena, Germany).

**2.6. Alkaline Single-Cell Gel Electrophoresis (Comet Assay):**

**Reagent:** 1 % Normal agarose, 100 mg normal agarose was added to 10 ml PBS and then heated until the agarose dissolved, 1 % Low melting agarose, 100 mg low melting agarose was added in 10 ml PBS and then heated until the agarose dissolved.

Electrophoresis buffer

NaOH (300mM) - 12 g,  $\text{Na}_2\text{EDTA}$  (1mM) - 372 mg. The volume was made to 1 litre with distilled water.

Neutralization buffer 12.11 g Tris (400mM) was dissolved in 250 ml of distilled water.

The above ingredients were added to 700 ml distilled water and dissolved. About 12 g pelletized NaOH was added in small quantities and stirred until the added salts dissolved completely into the solution. The pH of the solution was adjusted to 10.0 using 0.1N HCl or NaOH and then made up to 990 ml with distilled water, filter-sterilized and stored at room temperature [16].  $10\text{ml}$  of Triton X -100 (1%) was added to the above solution and refrigerated for 30 - 60 min prior to use. Ethidium bromide,  $5\mu\text{l}$  of ethidium bromide from the working solution was used [17].

Non-small cell lung carcinoma cell line (NCI-H460) were used for the study. Cells in  $T_{25}$  flasks

were trypsinized and pelleted. The pellets were washed thrice.

**Cell Lysis:** After solidification of the agarose, the cover slips were removed and the slides were immersed in ice-cold lysis solution and placed in a refrigerator at 4°C for 16h[18]. All the above operations were performed in low lighting conditions in order to avoid additional DNA damage.

**Electrophoresis:** After removing the slides from the lysis solution, they were placed horizontally in an electrophoresis tank[19]. The reservoirs were filled with electrophoresis buffer until the slides were just immersed in it. The slides were allowed to stand in the buffer for about 20 min (to allow DNA unwinding) after which electrophoresis was carried out at 0.8 V/cm for 15 min. All statistical analyses were made using SPSS 11.0 software package (SPSS, Tokyo, Japan). After electrophoresis, slides were removed, washed thrice in neutralization buffer and gently dabbed dry. A few drops of the working solution of ethidium bromide were added on to the gel and the slide was covered with a cover slip. The stained DNA in the cells were examined at 200x and 400x magnifications using a fluorescent microscope equipped with a 365 nm excitation filter and a 435 nm barrier filter. The length of the DNA migration (comet tail) in these cells was measured directly by fixing an ocular micrometer in one of the eyepieces of the microscope. About 60 - 100 comets were scored per point. One hundred cells from each treatment group were digitalized and analyzed using Comet Assay Software Programme (CASP). The images were used to estimate the DNA content of individual nuclei and to evaluate the degree of DNA damage representing the fraction of DNA in the tail and other comet parameters.

### 2.7. Statistical Analysis:

Data were analyzed by one-way analysis of variance (ANOVA) and a significant difference among treatment groups were evaluated by Duncan's Multiple Range Test (DMRT). The results were considered statistically significant at *P* value less than 0.05. All statistical analyses were made using SPSS 11.0 software package (SPSS, Tokyo, Japan).

## 3. Results and Discussion

### 3.1. Optimization for AgNp Production:

Addition of various concentration of AgNO<sub>3</sub> to *Nocardia mediterranei*-5016 pellet and supernatant led to change in color change at 1 mM concentration of AgNO<sub>3</sub> which was added to the pellet. It shows that 1Mm is the optimum concentration required for AgNp production.

There was no color change observed in supernatant when AgNO<sub>3</sub> was added to it. This shows that the pellet has the ability to convert AgNO<sub>3</sub> to AgNp. This was primarily observed by taking reading in UV-spectrophotometer at 420 nm in 1mM concentration.

### 3.2. UV Spectrophotometer Analysis:

The primary detection for synthesis of nanoparticle is done by UV Spectroscopy. A surface Plasmon peak located at interval of 400-420 nm was observed for the AgNp production from *Nocardia mediterranei*. It is found that the Ultraviolet detection of Silver nanoparticles consist of few humps. These humps show that the molecule is absorbing radiation over a band of wavelengths. One reason for this band was observed because of electronic level transition which was usually accompanied by a simultaneous change between the more numerous vibrational levels. (Fig. 1) shows the absorption spectra of Silver nanoparticle produced by *Nocardia mediterranei*.

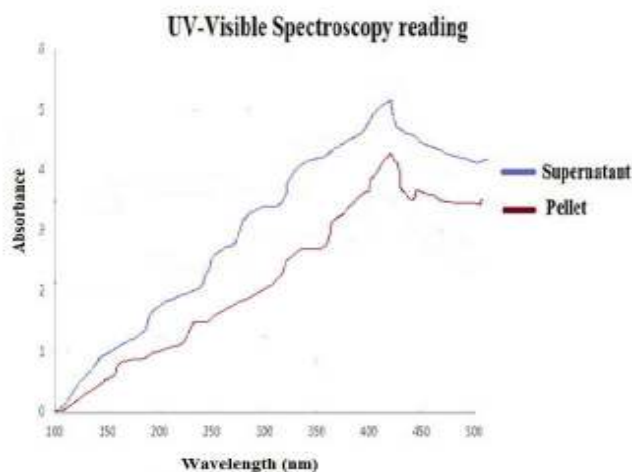


**Fig. 1: The absorption spectrum of Silver nanoparticles synthesized by *Nocardia Mediterranei***

### 3.3. FT-IR Analysis

Figure 2 shows FTIR spectra of synthesized Ag NPs by using *Nocardia meditteranei* and found strong bands at  $3427.51$ ,  $1010.70$   $\text{cm}^{-1}$  corresponds to stretch in OH band ( $3200$ - $3600$ ). The level of C=O ranges from  $1647.21$  to  $1739.79$   $\text{cm}^{-1}$ . The peaks  $3736.12$ ,  $3427.51$  and  $3412.08$  shows the presence of absorbance at amine (N-H) region. The peak  $2974.23$  represents stretch at C-H. The peak at  $1641.42$  shows presence of  $\text{C}=\text{C}$ -region. The peak value obtained for C-N region is  $1286.52$ . The occurrence of a spectrum over wavelength range of  $1200$ -  $1000$   $\text{cm}^{-1}$  indicates the presence of the polysaccharide in the synthesized nanoparticles. Fourier transform infrared spectroscopy demonstrated that the chemical of nanoparticles synthesized by *Nocardia meditteranei* was non homogenous.

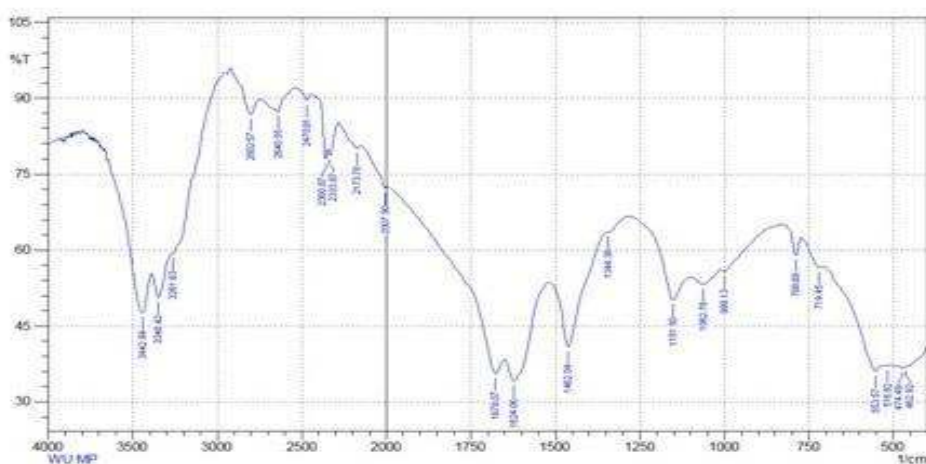


**Fig. 2: FTIR analysis of Silver nanoparticles produced by *Nocardia Meditteranei*.**

### 3.4. Microscopic Analysis of biologically synthesized Silver nanorods

Scanning Electron Microscope (SEM) and Transmission Electron Microscope (TEM) analysis revealed the morphology and size of the synthesized silver nanorods. SEM imaging showed rod shaped particles and TEM image of Biologically synthesized silver nanoparticles at  $10,000\times$  showed  $49.98$  nm sized particles (Fig. 3).

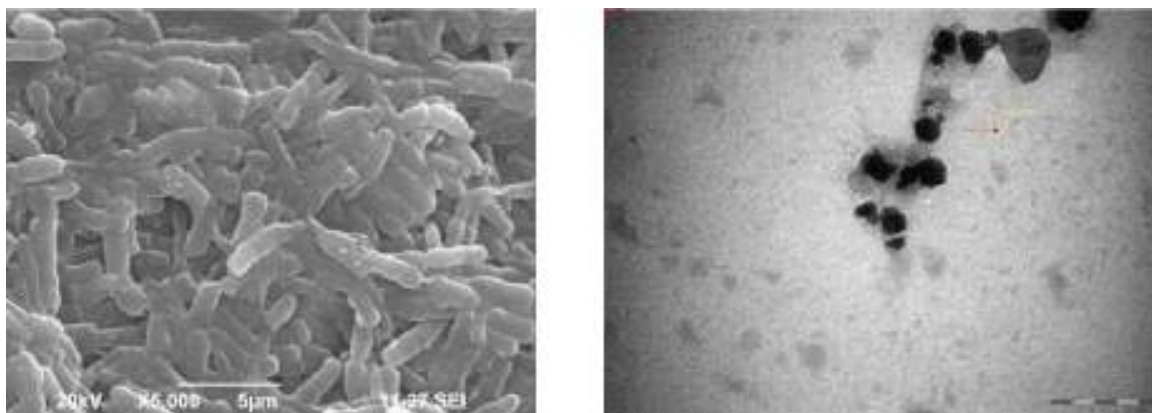


**Fig. 3: Microscopic analysis of synthesized silver nanorods (a) SEM imaging (b) TEM imaging**

**3.5. *Invitro* Cytotoxicity:**

Mitochondrial function-based MTT conversion to formazon crystals (MTT assay) is often used as cell viability test in cell culture system. In the present study silver nanorods exerted cytotoxic effects on non-small cell lung carcinoma cell line (NCI-H460) at the concentration of 2-20µg for a period of 24h, 48h and 72h. Nanorods inhibited the growth of the non-small cell lung carcinoma cell line (NCI-H460) significantly in a dose and time dependent manner. The cytotoxic activity of this cell line was determined based on the concentrations of the compound required to reduce the survival of cells by 50% (IC<sub>50</sub>). Nanorods were highly cytotoxic to the non-small cell lung carcinoma cell line (NCI-H460) were at very low concentrations and IC<sub>50</sub> dosage is differ in time and dose dependent manner. The IC<sub>50</sub> values for nanorods are shown in Table 1 and Figure 4 shows the MTT assay for non-small cell lung carcinoma cell line (NCI-H460). Since nanorods at a dose 11.68µg were found to be effective for 24h treatment it was fixed for further analysis.

**Table 1: IC<sub>50</sub> values of nanorods on non-small cell lung carcinoma cell line (NCI-H460).**

| Cell line (Nanorods IC <sub>50</sub> (µg)) | 24h   | 48h  | 72h  |
|--|-------|------|------|
| NCI-H460                                   | 11.68 | 7.93 | 4.15 |

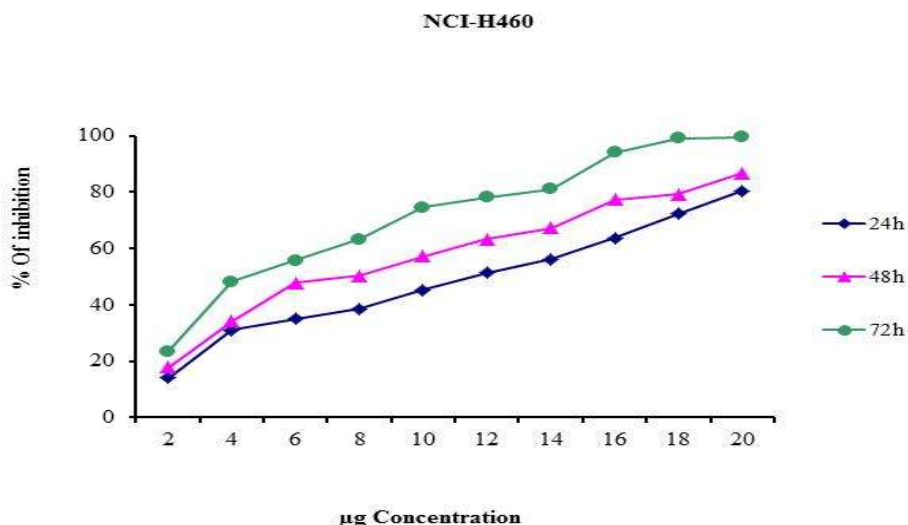


**Fig. 4: MTT assay of nanorods treated human non-small cell lung carcinoma cell line (NCI-H460).**

### 3.6. Effect of Nanorods on Cell Morphology:

The effects of nanorods at a fixed  $IC_{50}$  dose on cultured non-small cell lung carcinoma cell line (NCI-H460) were evaluated by exposing the cells for 24h and 48h. Bright field microscopic analysis with untreated control and treated cells revealed that  $IC_{50}$  dose of nanorods induced changes in cellular shape. Most of the cellular contents were found as small fraction so the cells became more granular in appearance. Due to the presence of swelling in their cytoplasm and colony morphology was less well defined. There were dissemble gaps between neighboring cells and remaining adherent cells had become more rounded which are characteristics of apoptosis, that confirming the cell death in a time dependent manner is represented in the Figure 5.

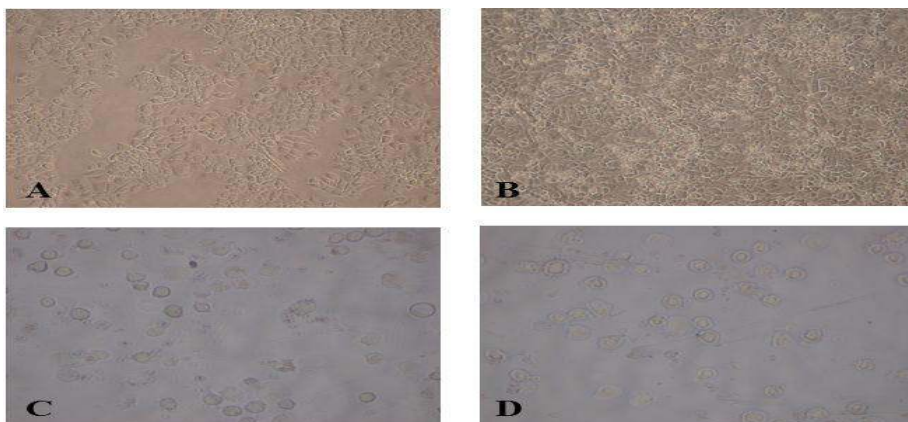


**Fig. 5:** Effect of nanorods  $IC_{50}$  levels on non-small cell lung carcinoma cell line (NCI-H460). A and B: 24h and 48h control groups showed normal cellular morphology. C and D: 24h and 48h  $IC_{50}$  nanorods treated groups showed dissemble gaps, granular in appearance and many death cells.

### 3.7. Effect of Silver Nanorods on Cell Cytochemistry using Hoechst 33258 staining:

The effect of nanorods on apoptotic induced morphological changes, the cells were first treated with the respective  $IC_{50}$  doses for 24h and 48h, stained with Hoechst 33258 and were observed under a fluorescent microscope (Fig. 6). The results showed that cells treated with nanorods exhibited apoptotic characteristics including marginalization and/or fragmentation of chromatin, bi-nucleation, cytoplasmic vacuolation, cell shrinkage, nuclear swelling, cytoplasmic blebbing and membrane integrity loss or deformation of late apoptosis indication of dot-like chromatin in the human primary colon cancer cells. These cytological changes indicate that the cells were committed to specific mode of cell death, either apoptosis or necrosis. Chromatin condensation was observed to increase in a time dependent manner with more number of cells susceptible at 48h.

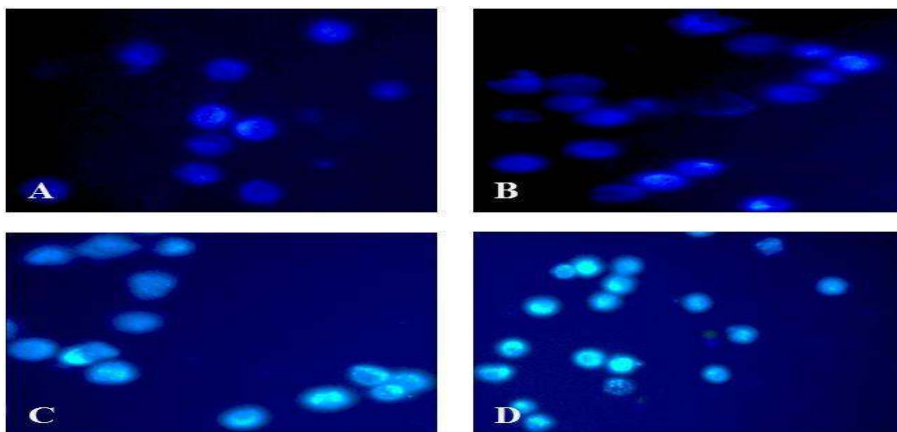


**Fig. 6:** Effect of nanorods on human non-small cell lung carcinoma cell line (NCI-H460) stained with Hoechst 33258. A and B: 24h and 48h control groups showed normal cells. C and D: 24h and 48h  $IC_{50}$  nanorods treated groups showed membrane integrity loss, nuclear swelling and dot-like chromatin fragmentation.

### 3.8. Effect of Nanorods on DNA Damage:

The induction of DNA strand breaks in cultured human primary cells by nanorods after 24 h and 48 h of incubation at IC<sub>50</sub> concentrations was assessed. The DNA damage in the treated cells was evaluated using single-cell gel electrophoresis (comet) assay as described in the protocol and stained with EtBr. Comet cells were scored and histograms were also prepared using comet analysis software (CASP). The nuclear head, comet parameters (tail length, % DNA in tail and olive tail moment) were recorded for 25 individual cells and comparative data were generated. DNA was observed in cells treated with nanorods after 24h incubation whereas the percentage of damaged cells increased on treatment with this compound for 48 hrs which was shown by the appearance of prominent comets with tail. The differences between the untreated and treated cells were viewed under a fluorescent microscope (Fig.7).

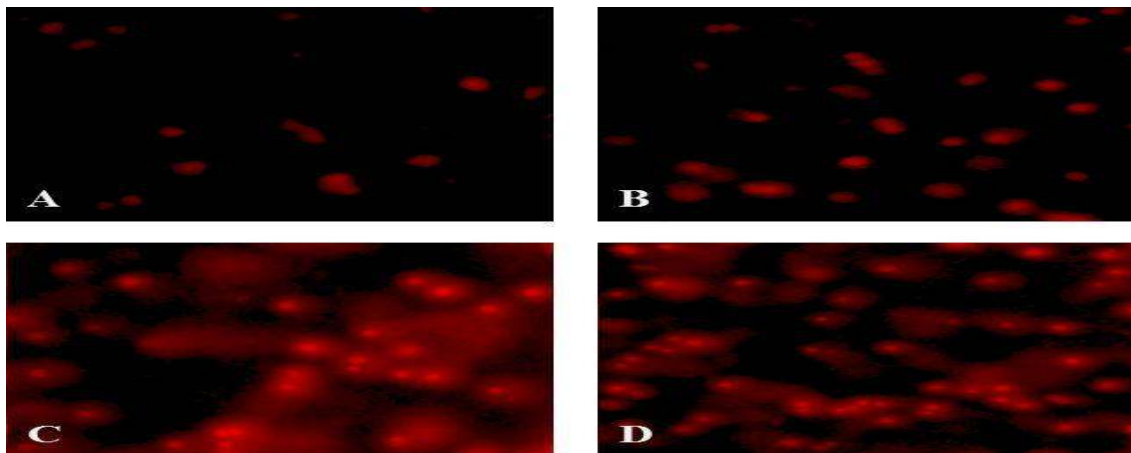


**Fig. 7:** Effect of nanorods on human non-small cell lung carcinoma cell line (NCI-H460) stained with ethidium bromide (Comet assay). A and B: 24h and 48h control groups showed intense green fluorescence C and D: 24h and 48h IC<sub>50</sub>carvone treated groups showed the progressive loss of green fluorescence.

**Table 2:** Effect of nanorods on various comet parameters on human non-small cell lung carcinoma cell line (NCI-H460).

| Groups |                | Tail length<br>(arbitrary units) | Tail DNA (%)            | Olive tail moment<br>(arbitrary units) |
|--------|----------------|----------------------------------|-------------------------|--|
| 24h    | Control        | 9.88±0.61 <sup>a</sup>           | 5.88±0.44 <sup>a</sup>  | 4.25±0.34 <sup>a</sup>                 |
| 48h    | Control        | 11.72±0.84 <sup>a</sup>          | 6.72±0.37 <sup>a</sup>  | 4.41±0.28 <sup>a</sup>                 |
| 24h    | Carvon treated | 61.45±5.60 <sup>b</sup>          | 27.94±2.31 <sup>b</sup> | 16.85±1.50 <sup>b</sup>                |
| 48h    | Carvon treated | 65.24±3.95 <sup>bc</sup>         | 28.35±2.35 <sup>b</sup> | 17.72±1.28 <sup>b</sup>                |

Data are presented as the means ± S.D. of 25 cells in each group. Values not sharing a common superscript letter (a-c) differ significantly at p<0.05 (DMRT).

### 3.9. Measurement of intracellular ROS by spectrofluorimetric method:

ROS was measured by using a non-fluorescent probe, 2,7-diacetyl dichlorofluorescein (DCFH-DH) that can penetrate into the intracellular matrix of cells where it is oxidized by ROS to fluorescent dichlorofluorescein (DCF) [20]. The percentage of ROS was estimated in the control and nanorods treated groups in time dependent manner 24h 48h respectively. Briefly, an aliquot of the above mentioned isolated cells (8×10<sup>6</sup> cells/ml) were made up to a final volume of 2 ml in normal phosphate buffered saline (pH 7.4). An 1 ml aliquot of cells were taken to which 100 µl DCFH-DA (10 µM) was added and incubated at 37°C for 30 min.

Fluorescent measurements were made with excitation and emission filters set at 480 nm excitation and 530 nm emission respectively (Shimadzu RF-5301 PC spectrofluorimeter). Results were expressed as percentage increase in % fluorescence intensity.



### 3.10. Study for ROS:

Figure 8 shows the levels of ROS generation in different treatment groups. There was a significant increase in the ROS levels in non-small cell lung carcinoma cells (NCI-H460) during nanorods treatment in time dependent manner. Increased ROS generation during nanorods treatment showed an additive effect of this particle in NCI-H460 cells. 48h (83.5%) treatment group showed more pronounced effect as compared to 24h (74.6%) treatment group it may be due to the enhanced treatment time of the nanorods in NCI-H460 cells.

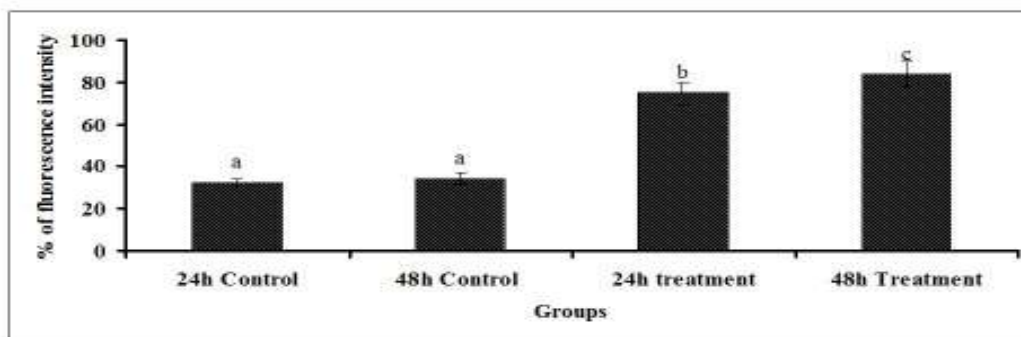


**Figure 8: Effect of nanorods in ROS generation. The generation of ROS levels during nanorodstreatment was measured spectrofluorimetrically by DCFH-DA staining. Values are given as means  $\pm$  S.D. of six experiments. Values not sharing a common marking differ significantly at  $P < 0.05$  vs. control (DMRT).**

## 4. Conclusion

In this study, AgNPs were synthesized by the secondary metabolites of *NocardiaMediterranei*-5016. Silver nanorods has found wide applications in semiconductor andmedical fields. Brown colour production was the evident that the cultures produce enzymesand reduce Silver nitrate to Silver ions. Biological synthesis of silver nanorods acquires special importance due to its inherent ecofriendly in nature. Basically synthesis of silver nanorods confirmed through the UV Vis Spectrophotometer reading which was obtained in between at the range of 400-450nm. Fourier transform infrared spectroscopy demonstrated that the chemical nature of nanorods synthesized by *Nocardia Mediterranei* was non homogenous. The various types of the bonds and stretches present in the AgNp has been studied using FTIR. The size of the silver nanorods has been detected by SEM analysis. The nanorods obtained have shown bactericidal effect against some pathogens. The synthesized Ag nanorods was effective against Non-small cell lung carcinoma cell line (NCI-H460), which was confirmed by MTT assay. The death of cancer cells was identified by Hoechst staining. The anticancerous activity of Ag nanorods have revealed a new way for curing cancer using nanorods. This Ag nanorods can be used for drug targeting and drug delivery.

**Acknowledgement:** Authors thankful to Management, Principal, and Head, Department ofBiotechnology of K.S.R. College of Technology, Mr. R. Vinoth Kumar Annamalai University, Karpagam University, NCIM Pune and Karunya University for providing the facility to carry out the research work.

## References

1. Ahmad, A., Mukherjee, P., Senapati, S., Mandal, D., Khan, M.I., Kumar, R., Sastry, M., Extracellular biosynthesis of silver nanoparticles using the fungus *Fusarium oxysporum*, Colloids and Surfaces, B: Biointerfaces, 27 (2003) 313-318.
2. AshaRani, P.V., Prakesh Hande, Suresh Valiyaveettil, M., Anti-Proliferative activity of Silver nano particles, BMC Cell Biology, 10 (2009) 65-67.
3. Fouzia, B., Ezhilarasan, M., Dr. Arumugam, Dr. Sahadevan, Green synthesis of silver particle from clemone viscosa synthesis and antibacterial activity, International conference on Bioscience, 5 (2011) 334-335.

4. Benjanin, Barathwaj, Onion (*Allium cepa*) as a potential candidate for silver nanoparticle synthesis and estimating its antibacterial activity, International Journal of Bioscience and Biochemistry, 4 (2011) 56-58.
5. Cai, W., Hsu, A.R., Li, Z.B., Are quantum dots ready for in vivo imaging in human subjects?, Nanoscale Res Letter, 2 (2007) 265–281.
6. Greider, C.W., Blackburn, E.H., Telomeres telomerase and cancer, Scientific American, 274 (1996) pp.80–85.
7. Huang, X., IH El-Sayed, Qian, W., Cancer cells assemble and align gold nanorods conjugated to antibodies to produce highly enhanced, sharp and polarized surface Raman spectra: a potential cancer diagnostic marker, Nano Lett 7 (2007) 1591–7.
8. Kalimuthu, K., Babu, S.R., Venkataraman, D., Bilal, M., Gurunathan, S., Biosynthesis of silver nanoparticles by *Bacillus licheniformis*, Colloids Surfaces, Biointerfaces, 65 (2008)150-153.
9. Kathiresan, K., Manivannan, S., Nabeel, A.M., Dhivya, B., Studies of nanoparticles synthesized by a marine fungus *Penicillium fellutanum* isolated from coastal mangrove sediment, Colloids Surfaces B: Biointerfaces, 71 (2009) 133-137.
10. Liu, Y., Shipton, M.K., Ryan, J., Synthesis, stability and cellular internalization of gold nanoparticles containing mixed peptidepoly(ethylene glycol) monolayers. Anal Chem, 79 (2007) 2221–9.
11. Mamadou diallo, Ahmad, A., Mandal, D., Senapati, S., Sainkar, S.R., Khan, M.I., Fungus Mediated synthesis of silver nanoparticles and their immobilization in the mycelial matrix: a novel biological approach to nanoparticle synthesis, Nano Lett., 1 (2001) 515-519.
12. Minaeian, S., Shahverd, A.R., Nohi, A.S., Shahverd, H.R., Extracellular biosynthesis of silver nanoparticles by some bacteria, Journal of Sciences, 17 (2008) 66.
13. Mohan puria, Ahmad Reza Shahverdi, Hamid Reza Shahverdi, Mohammad Reza Khorramizadeh, Ahmad Reza Gohari, Green synthesis of small silver nanoparticles using geraniol and its cytotoxicity against fibrosarcoma, Avicenna Journal of Medical Biotechnology, 1 (2009) 2.
14. Mona Safaepour, Ahmad Reza Shahverdi, Hamid Reza Shahverdi, Mohammad Reza Khorramizadeh, Ahmad Reza Gohari, Green synthesis of small silver nanoparticles using geraniol and its cytotoxicity against fibrosarcoma, Avicenna Journal of Medical Biotechnology, 1 (2009) 2.
15. Mritunjai singh, Shijini singh, Prasad, S.A., Ghambir, I.S., Synthesis of plant-mediated silver nanoparticles using papaya fruit extract and evaluation of their anti microbial activities, Digest Journal of Nanomaterials and Biostructures, 4 (2008) 557-563.
16. Park, J.W., Benz, C.C., Martin, F.J., Future directions of liposome and immunoliposome-based cancer therapeutics, SeminOncol, 31 (2004) 196–205.
17. Parkin, D.M., Pisani, P., Ferla, J., Estimates of the worldwide incidence of 25 major cancers in 1990, Int J Cancer, 80 (1999) 827–41.
18. Balagurunadhan, R., Radhakrishnan, M., Baburajendaran, R., Biosynthesis of gold nanoparticles by actinomycetes *streptomyces viridogens* strain HM 10, Indian Journal of Biochemistry and Biophysics, 48 (2011) 331-335.
19. Murali, S., Ahamad, A., Islam Khan, M., Raji, K., Biosynthesis of metal nanoparticle using Fungi and actinomycetes, Current science, 85 (2003) 22-25.
20. Jesudason, E.P., Masilamoni, E.G., Charles Jebaraj, E.J. Solomon, F.D., Jayakumar, R.P., Efficacy of DL-a lipoic acid against systemic inflammation induced mice Antioxidant defense system, Mol. Cell. Biochem, 313 (2008) 113–123.
21. Saiffudin, C.W. Wong, Nur Yasumira, Rapid biosynthesis of silver nanoparticles using culture supernatant of bacteria with microwave irradiation, Journal of Chemistry, 6(1) (2009) 61-70.

\*\*\*\*\*